Les sables de Fontainebleau: A Natural Quartz Reference Sample and its Characterisation

Sebastian Kreutzer,[1*] Johannes Friedrich,[2] David Sanderson,[3]
Grzegorz Adamiec[4], Alicja Chruścińska[5], Mauro Fasoli[6,7],
Marco Martini[6,7], George S. Polymeris[8], Christopher I. Burbidge[9] & Christoph Schmidt[2]

[1] IRAMAT-CRP2A, Université Bordeaux Montaigne, Pessac, France

[2] Chair of Geomorphology & BayCEER, University of Bayreuth, Bayreuth, Germany

[3] SUERC, Scottish Enterprise and Technology Park, East Kilbride, Scotland, UK

[4] Institute of Physics CSE, Silesian University of Technology, Gliwice, Poland

[5] Institute of Physics, Faculty of Physics, Astronomy and Informatics, Nicolaus Copernicus University, Torun, Poland

[6] Dipartimento di Scienza dei Materiali, Università degli Studi di Milano Bicocca, Milano, Italy

[7] INFN, Sezione di Milano Bicocca, Piazza della Scienza 1, I-20126 Milano, Italy

[8] Ankara University, Institute of Nuclear Sciences, Ankara, Turkey

[9] Office of Radiation Protection and Environmental Monitoring, Environmental Protection Agency, Dublin, Ireland

[*]Corresponding Author: sebastian.kreutzer@u-bordeaux-montaigne.fr

---

Abstract

Fundamental studies on luminescence production in natural quartz require samples which can be studied by groups of laboratories using complementary methods. In the framework of a European collaboration studying quartz luminescence, a sample originating from the Fontainebleau Sandstone Formation in France was selected for characterisation and distribution to establish a starting point for interlaboratory work. Here we report on the preparation and characterisation work undertaken before distribution with the aim of ensuring that each laboratory received comparable material. Material was purified to enrich the quartz concentration, followed by mineralogical screening by SEM and ICP-MS analyses. Luminescence screening measurements were undertaken at a single laboratory (SUERC) to verify the suitability of the sample for use within the study, and to establish the level of homogeneity of subsamples prepared for distribution. The

sample underwent minimal non-chemical pre-treatment by multiple cycles of magnetic separation and annealing. SEM analysis showed that the sample consists mainly of SiO_2. The luminescence characterisation confirmed a dose sensitivity of ca. 22,000–160,000 cts K^{-1} Gy^{-1} per 260–290 grains for the 110 °C UV TL peak, well developed low (here: 100–300 °C) temperature (pre-dose) TL signals and high OSL sensitivities. The grain to grain OSL response varies by more than one order of magnitude. No significant IRSL signal was observed. In summary, the results from luminescence characterisation confirm the suitability of the sample for the luminescence experiments envisaged and have established a basis for comparability in studies conducted by a network of laboratories.

Keywords: OSL, TL, Characterisation, Fundamental research

1. Introduction

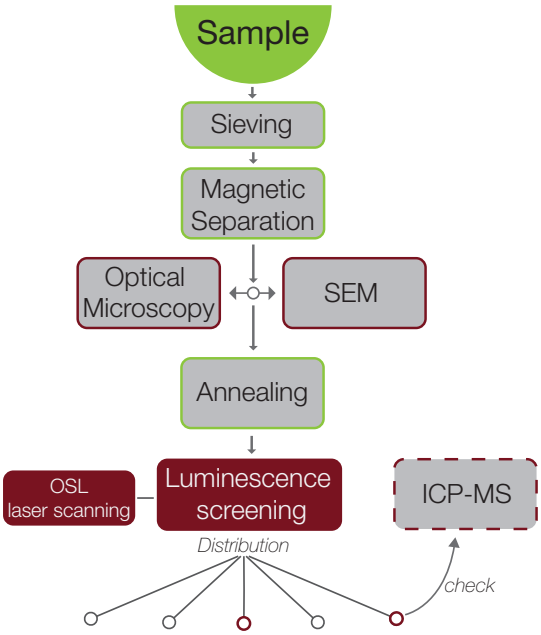

Figure 1. Flowchart of the sample treatment and applied screening procedures. The ICP-MS analysis was carried out on one subsample only.

Fundamental studies on quartz luminescence characteristics dedicated to dosimetric applications quickly reach a point where (natural) reference samples are needed. Such samples ideally would (1) enable reproducible experiments to be conducted within individual laboratories to help set up procedures, (2) provide material which could be used as a control sample for work with a range of different samples, and (3) provide a traceable means of assimilating data from different laboratories, providing the homogeneity has been adequately established. The requirements for such materials were discussed in the framework of a European collaboration at meetings in Bayreuth, Torun and Glasgow, where it was concluded that natural quartz samples of high purity were needed to established interlaboratory comparability. Materials with high dose sensitivity (110 °C single grain peak intensity > 100 cts K^{-1} Gy^{-1}), good signal reproducibility (e.g., TL peak shape), minimal preceding chemical treatment and availability in large quantities (> 500 g) were required, and the importance of characterisation in a single laboratory and careful partition and distribution were recognised. In the longer term, it may be necessary to develop a series of such materials

from different natural settings, to reflect a broader range of quartz luminescence characteristics as well.

Some previous studies have used samples initially obtained from dating studies as model systems (e.g., Wintle & Murray, 1997; Bailey, 2000; Gong et al., 2014), others have used commercially available bulk material (e.g., Keleş et al., 2016), quartz extracted from the bedrock (e.g., Friedrich et al., 2017) or a mixture of such samples (e.g., Adamiec, 2005). However, the information on origin, pre-treatment and mineralogical characterisation and homogeneity differ in these examples, and basic luminescence characteristics appear to be only rarely reported, or if given, spread over several articles. Here we report the characterisation and preparation of a quartz derived from the Fontainebleau sands, undertaken at the Scottish Universities Environmental Research Centre (SUERC) prior to distribution to the working group. This material has subsequently been used in an interlaboratory study of the kinetic parameters of the 110 °C TL signal, and it is intended that it should also be used for future experiments on luminescence production of quartz within the group.

Chemical composition screening using a scanning electron microscope (SEM) was used to ensure the purity of the quartz sand and inductively coupled plasma mass spectrometry (ICP-MS) analyses were conducted to obtain information on trace elements. We furthermore present a brief and easily to apply luminescence pre-characterisation routine using thermally stimulated luminescence (TL) and optically stimulated luminescence (OSL) measurements. Additional OSL laser scanning investigates the grain to grain variation in luminescence response.

The characterisation and homogeneity testing reported here have been used in formal interlaboratory validation studies (e.g., Sanderson et al., 2003a,b,c,d), but do not seem to have been adopted to the same extent, so far, in geochronological applications of luminescence methods. However, we believe that such (pre-) characterisation is indispensable to avoid ambiguities later in the research project. It is furthermore a cornerstone to combine research results from different labs, without worrying about the sample to sample differences biasing the conclusions. We structured the manuscript as a workflow paper, with information on the equipment used given in the corresponding sections. The general preparation and characterisation workflow is shown in Fig. 1.

2. Sample origin and description

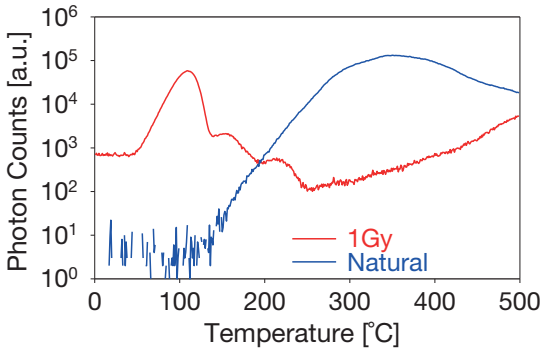

Figure 2. Thermoluminescence glow curves from the quartz fraction before annealing. Net curves after reheat subtraction recorded at 5 K s^{-1} using a SUERC manual TL reader from the natural signal and a 1 Gy regenerated signal.

The material selected originates from the Oligocene Fontainebleau Sandstone Formation (Formation des Sables de Fontainebleau) in France. These sediments were deposited during the time of the last marine intrusion into the Paris Basin (the Stampian Sea, or Sea of Estampes) ca. 35 Ma ago (e.g., Grisoni & Thiry, 1988). The sand itself is usually extracted in large quantities by

surface mining from a coastal palaeo-dune system, which reaches a mean thickness of ca. 50 m (max. 100 m; Thiry & Marechal 2001). Thiry & Marechal (2001) distinguish three diagenetic facies: (1) plateau sands and sands at the edge of valleys, which are almost composed of pure quartz, (2) sands beneath the plateaus containing clays and traces of feldspars and (3) sands from below the water-table containing, amongst others, feldspar, carbonates and organic matter. For more detailed information see El Bied et al. 2002; Thiry & Marechal 2001; Robin & Barthélemy 2000; Grisoni & Thiry 1988. Due to its high purity (quartz concentration $> 99\,\%$; e.g., Saadi et al. 2017; Thiry et al. 1985; Bourbie & Zinszner 1985), Fontainebleau sand is preferred in industrial glass production. After mining, the sand for this purpose undergoes a pre-treatment, consisting mainly of chemical washing and density separation (cf. Bouniol, 2013).

Five kilograms of the 'Sable de Fontainebleau' were purchased in 2005 by SUERC from Merck Eurolab (nowadays: *VWR*). The material was characterised together with a series of other commercial quartz samples, to select materials which could be sensitised for use as OSL-D materials. This preliminary screening work confirmed that the material had high sensitivity TL and OSL with well-defined low temperature ($< 300\,^{\circ}$C) and high-temperature TL ($> 300\,^{\circ}$C) peaks. Both OSL and the low-temperature TL signals exhibit pre-dose sensitisation. A retained portion of 800 g of the sieved 150–250 μm fraction was available at SUERC, and this was selected for this study. The supplier label of the material did not include specific batch numbers or give details of the Merck processing of the product before purchase.

However, TL and OSL analysis of the raw input material, as well as the sieved fractions, shows the presence of geological residual signal. The presence of this residual geological signals in the material had been noted in the exploratory work conducted by Burbidge in 2005 (unpublished). Figure 2 shows the TL signals associated with this geological dose, and the shape of a 1 Gy regenerated response recorded with a manual TL reader at SUERC. It displays the high temperature residual signal (equivalent dose approximately 400–500 Gy based on the 340–360 $^{\circ}$C signal integral) and the response to a 1 Gy dose read without preheat. The curves are net curves following reheat. The natural curve confirms that the sample had not been significantly heated prior to receipt, gives an indication of the shape of the high temperature TL signals, and suggests that deeper trap signals above 500 $^{\circ}$C may also be present. The regenerated curve shows initial phosphorescence, the post irradiation delay being approximately 300 s and the low temperature peaks corresponding to nominal 110 $^{\circ}$C , 150 $^{\circ}$C and 210 $^{\circ}$C signals. All of these peaks respond to pre-dose sensitisation, whereas the sensitisation of the higher temperature (e.g., 325 $^{\circ}$C) peaks is minimal and hardly visible.

Additionally, high-resolution γ-ray spectrometry analysis was conducted on the raw material, but not published so far. For this, 100 g were counted for 50 ks on a shielded (50 % relative efficiency) Ortec Gamma-X spectrometer at the SUERC. Weighted analysis of the main U and Th series γ-lines were used to obtain activity per mass and concentration data (Table 1). See Sec. 8 for a discussion of these results.

3. Magnetic separation

Our sample preparation design for the Fontainebleau (FB) quartz aimed to avoid any chemical treatments. In particular, we did not treat the samples with HF, since we wanted to avoid modifications of the surface condition of quartz grains, or other malign effects on the grain shape (e.g., Porat et al., 2015). Visual inspection under low power optical microscopy revealed mainly milky and clear quartz grains, a few coloured grains and potentially some opaque heavy minerals. The latter contamination was hardly visible using optical microscopy (cf. Fig. 3). To remove heavy minerals without applying heavy liquids for density separation and to roughly quantify their abundance, a magnetic separator (Frantz, LB-1) was used to purify the sample further. Porat (2006) gives details on this method. The magnetic separation was performed using a current of 1.5 A for the magnetic

Table 1. High-resolution γ-ray spectrometry analysis results (bulk sample).

Source	**Activity**	**Concentration**
	[Bq kg^{-1}]	[ppm]
K	5.979 ± 4.413	190 ± 140
U	0.757 ± 0.202	0.061 ± 0.016
Th	1.369 ± 0.227	0.337 ± 0.056

Net data were derived after background subtraction and quantified relative to the SUERC Shap granite standard presented in a matched geometry. Quoted uncertainties combine sample, background and standard measurements, plus the uncertainties of the reference data. Sample counting statistics dominates the stated errors.

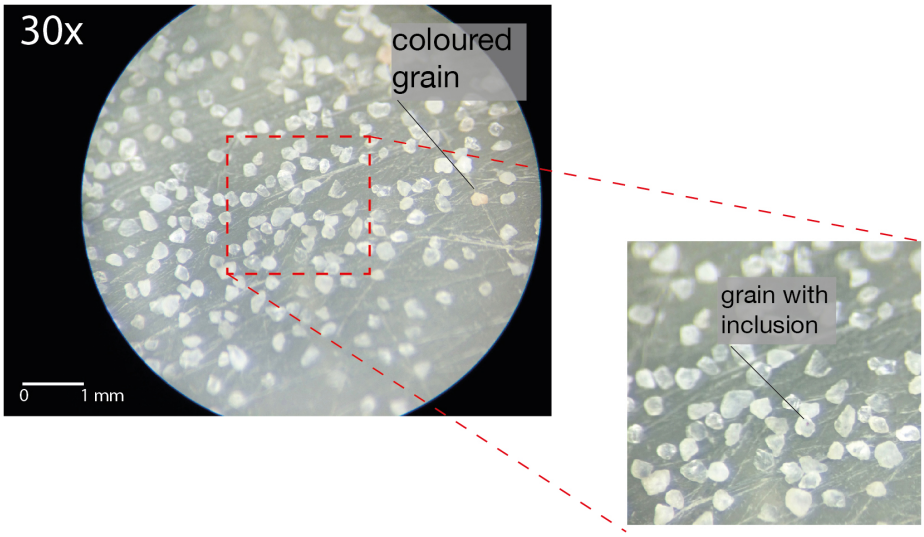

Figure 3. Pan view through an optical microscope with a magnification of 30 x. Note the grains with inclusions and coloured grains.

field (ca. 2 T), a slope of 7 ° and a tilt of 5 ° for the chute. After four runs with half of the available material, visual inspection showed that black or dark grains were slightly enriched (supposedly heavy minerals) in the separated magnetic fraction. Both fractions ('magnetic' and 'non-magnetic') were subsequently analysed using backscattered electron microscopy to see whether heavy minerals were present. The magnetic separation procedure was later repeated at least ten times, following a first SEM inspection using the fraction enhanced in magnetic grains.

4. SEM inspection

We used scanning electron microscopy in backscatter mode (using the Hitachi S-3400N SEM in the SUERC luminescence lab, electron beam: 20 keV), coupled to X-ray spot analysis (Oxford instruments INCA system) to manually analyse the magnetic fraction (suspected to be enriched in heavy minerals) and the purified non-magnetic fraction. However, no differences were found between the two fractions, and therefore they were not further separated for following analyses. Figures 4 and 5 summarise the results of the SEM inspection. We found mainly pure quartz grains with rounded and sub-rounded shapes,

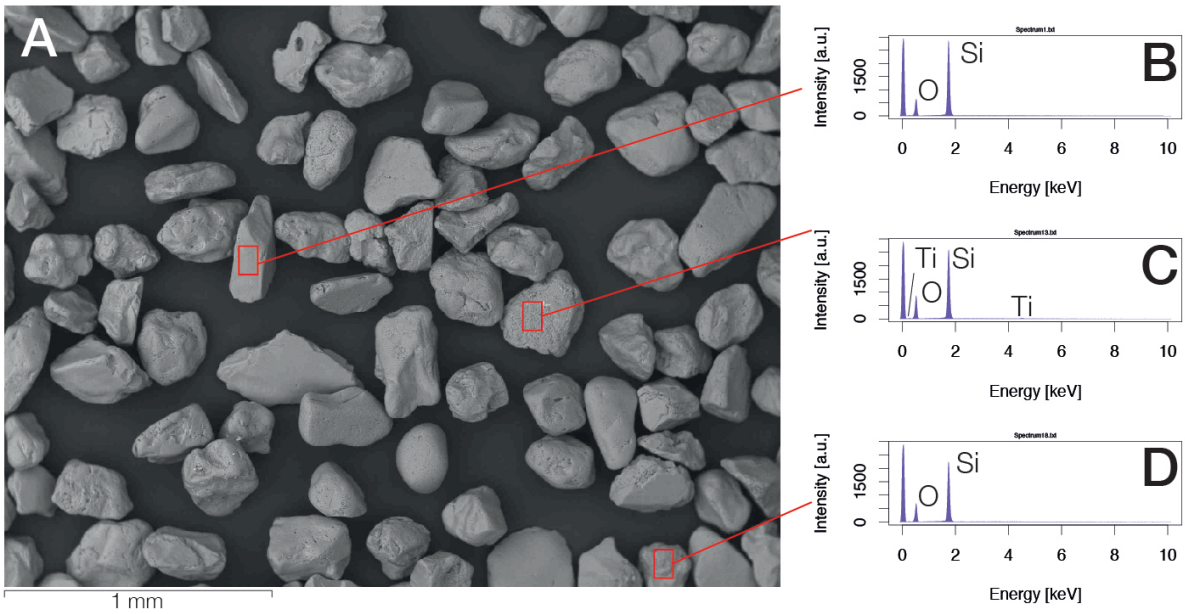

Figure 4. SEM pan view (A) and selected example spectra for three grains (B, C, D). No major impurities were observed.

although diverse forms and surface textures (sub-angular) were observed (cf. Powers, 1953, for a roundness scale). The observed grade of rounding is likely to reflect the diverse origin of the sample material. There was no substantial indication of effects from any prior chemical treatment by the supplier (cf. Figs. 4 and 5). The major elemental composition of the inspected grains was dominated by SiO_2. A small minority of grains showed Zr and Ti-bearing inclusions (Figs. 5A, 5C). We also found fragments of Ca and S (Fig. 5B), which are believed to remain from the sample pre-treatment by the supplier. Considering the constraints of the subsampling by SEM, qualitatively it can be said that the sieved sand is a high-purity quartz-dominated sample, as expected. The minor impurities and potentially diverse quartz textures are generally consistent with other work on the Fontainebleau Sandstone Formation (e.g., El Bied et al., 2002). No quantitative mineralogical analysis was performed.

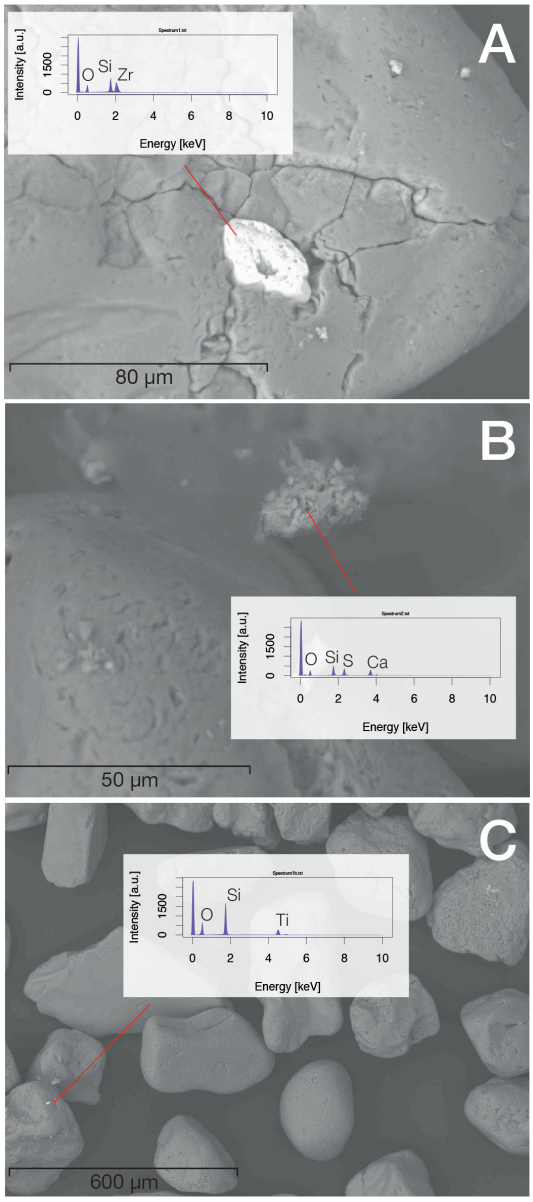

Figure 5. SEM close up. Three grains were exemplarily selected; detected major elements are indicated in the inset graphs. The following impurities were verified: Zr (A), Ca, S (B) and Ti (C). The majority (ca. 99 %) of the inspected grains consisted only of Si and O.

5. Annealing and packing

After SEM inspection, the sample material was annealed, in air, in a muffle furnace to remove residual luminescence signal. The material was annealed in a zirconium crucible, with closed lid, placed on a metal plate on ceramic pillars in the centre

of the preheated furnace. The temperatures of both the metal plate and the sample material were monitored using separate logged thermocouples. Figure 6 shows the temperature of the plate below the zirconium crucible and the temperature of the thermocouple embedded in the quartz sand sample. The furnace had been preheated to 470 °C before introducing the material. It took ca. 50 min before the sample temperature converged with the temperature recorded by the oven itself. In total, the sample was annealed for 82 min, while the temperature of the quartz itself was held at 490 °C for 30 min (indicated by the vertical lines in Fig. 6). Subsequently, the crucible was allowed to cool rapidly to room temperature outside the oven. This annealing cycle aimed to remove the geological TL and OSL signals without crossing the quartz α- to β-phase transition, and without fully depleting deep traps that might have de-sensitised the luminescence.

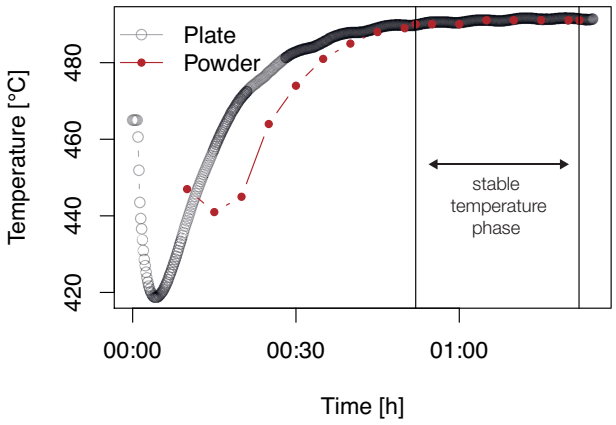

Figure 6. Temperatures recorded during annealing of the Fontainebleau quartz. Vertical lines indicate the time while the metal plate and the sample were held at similar temperatures for 30 min. The oven had been preheated to ca. 470 °C before loading. The sudden temperature decrease at the beginning was caused by the loading process.

After annealing, the sample material was homogeneously divided into ten batches packed into two tubes (A and B) of ca. 4 g each (in total twenty subsamples). While tubes labelled 'A' were distributed amongst the collaboration partners, tubes labelled with 'B' were retained at SUERC in case of loss in transit and for a later cross-check. A further quantity of unpacked annealed material has also been retained. Each of the 40 subsamples was then subject to luminescence screening to determine the extent of homogeneity prior to distribution.

6. Luminescence screening

6.1. Equipment

Before distribution, the luminescence properties of the annealed quartz samples were investigated. Two aliquots were prepared from each 'A' and 'B' subsample of the packed material, making a set of 40 aliquots in total. The grains were dispensed onto 9.6 mm diameter and 0.25 mm thick cleaned stainless steel discs using Electrolube Silicone Grease. It is estimated that the weighed aliquots comprised ca. 260–290 grains (estimated using the function `calc_AliquotSize()`; Burow 2017 from the **R** package 'Luminescence'). Measurements were done using a Risø DA-15 TL/OSL reader equipped with a ^{90}Sr/^{90}Y β-source

delivering ca. 0.1 Gy s^{-1} to quartz coarse grains (100–250 μm). Luminescence was recorded through a 7.5 mm Hoya U340 filter, while stimulating the sample either with blue LEDs (470 ± 5 nm at ca. 24 mW cm^{-2}) or an infrared laser (830 nm at ca. 90 mW cm^{-2}). The data analysis presented here was carried out using the **R** (R Core Team, 2017) package 'Luminescence' (Kreutzer et al., 2012, 2017). The **R** script used for analysing the luminescence measurements is provided as supplementary data.

6.2. Sequence

Two aliquots were prepared from each batch ('A' and 'B', 40 aliquots in total). Our rapid luminescence screening sequence comprised the following steps:

A. TL to 500 °C with 5 K s^{-1} (reader background subtraction)

   β-irradiation for 20 s ($\sim$ 2 Gy)

B. TL to 160 °C with 5 K s^{-1} (reader background subtraction)

C. IRSL at 50 °C for 20 s (60 % LED power)

D. OSL at 125 °C for 20 s (60 % LED power)

E. TL to 500 °C with 5 K s^{-1} (reader background subtraction)

6.3. Results

The summary of all measured curves is shown in Figs. 7A–E. The horizontal order follows the screening sequence (steps A to E). Each plot shows the results of all measured 40 aliquots. After annealing, first a TL residual measurement up to 500 °C was conducted. Fig. 7A reveals a small initial low-temperature TL signal at ca. 150 cts K^{-1} for 32 out of 40 measured aliquots. In contrast, the aliquot on position 1 (first measured aliquot) did not show this signal (Fig. 8, TL-initial, black curve). Thus, we conclude that irradiation cross-talk induced these small TL signals within the luminescence reader (e.g., Bray et al., 2002). The relative irradiation cross-talk of this signal is 0.045 ± 0.025 % and corresponds to the findings by Bray et al. (2002) (0.0055 ± 0.012 %).

In Fig. 7B the response of the so-called 110 °C UV TL peak following irradiation with a dose of ca. 2 Gy is shown. Exact peak positions vary from aliquot to aliquot, reflecting variations in thermal contact from disc to disc in the reader. The mean nominal temperature for this peak was 127 °C (range: 116 °C to 137 °C). The results show a 110 °C UV TL peak sensitivity of the material from ca. 22,000–160,000 cts Gy^{-1} for the ca. 260–290 grains (roughly 30,400 cts Gy^{-1} mg^{-1}) placed on each disc, if measured with a heating rate of 5 K s^{-1}. Further TL peaks (step E) were found at 200 °C (range: 187 °C to 219 °C) and 250 °C (mean: 248 °C, range: 230 °C to 276 °C). No further UV TL signal, e.g., at ca. 325 °C was found, presumably due to its lower sensitivity in comparison to the peaks at lower temperature.

All aliquots showed a weak IRSL signal in the UV-band (Fig. 7C). The weak correlation between the integrated OSL and IRSL signal of $r = 0.21$ (cf. Fig. S3, supplement) suggests that the IRSL signal is caused by mineral phases other than quartz. However, the IRSL signal is in 39 out of 40 cases < 1 % (mean: 0.4 %; extreme value: 1.5 %) of the corresponding blue-OSL signal (Fig. 7D) and with this considered being negligible. The signal integration range was similar for IRSL and OSL.

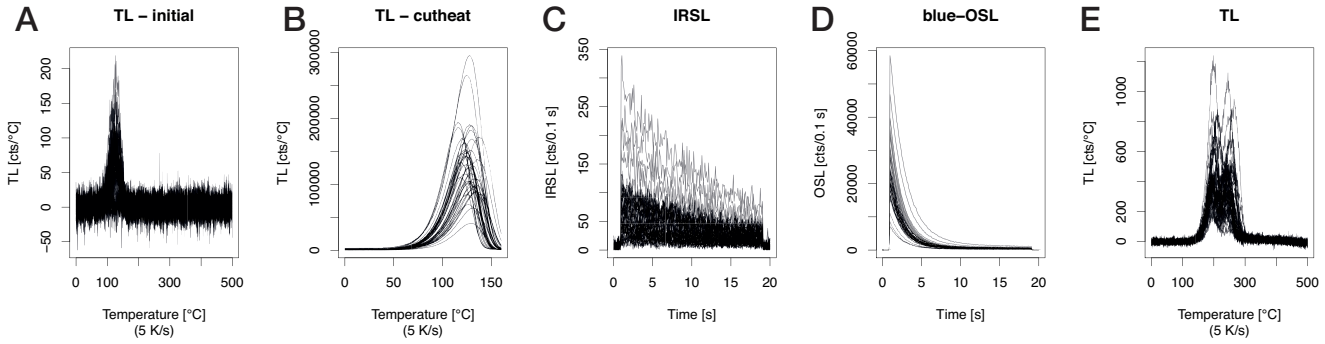

Figure 7. Luminescence screening results of the Fontainebleau quartz. Shown is a comprehensive plot comprising the signals of all measured aliquots (40 in total). The horizontal order of the plots follow the screening sequence (Sec. 6.1). The initial TL peak in (A) is believed to be induced by irradiation cross-talk within the luminescence reader. For further details see main text.

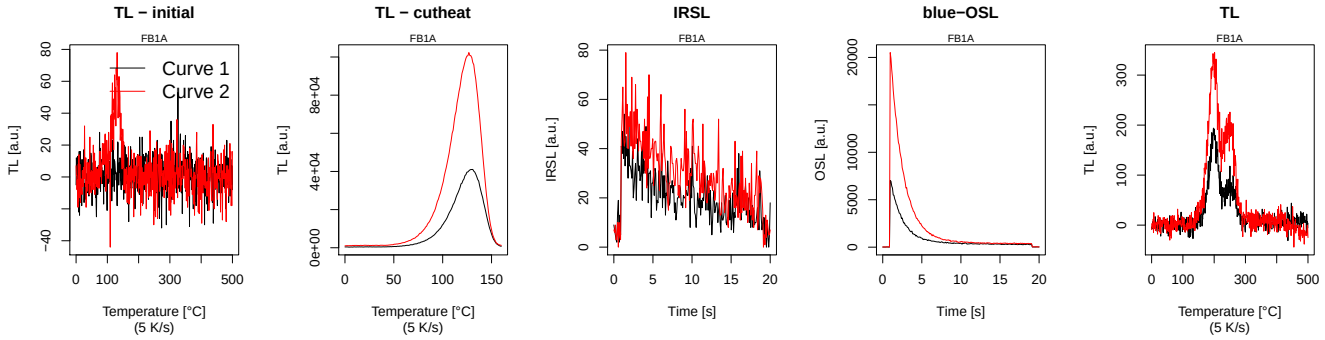

Figure 8. Luminescence screening results for one sub-sample (the first two aliquots measured). These results further emphasise that the small TL peak in Fig. 7A is likely resulting from cross-irradiation within the reader, since the first curve ever measured is unaffected. Intensity differences are believed to be usual inter-aliquot scatter.

6.4. Further analysis

The presented measurement data were used to further characterise the Fontainebleau quartz by post-processing. Of particular interest are: (A) TL peak position distribution, (B) TL peak intensity distribution, (C) TL peak intensity vs. IRSL intensity and (D) TL peak intensity vs. OSL intensity. The TL peak position was determined semi-automatically, selecting the intensity maximum of each peak in a given temperature range (1–220 °C and 230–500 °C). The peak intensity was derived from the sum of the intensity of the ±5 channels (1 channel := 1 K) around the maximum. The intensity values for the IRSL and blue-OSL signal were obtained from the full shine-down curves (no background subtraction) and plotted against the TL peak intensities on a logarithmic scale. The above described analysis was performed for all identified UV TL peaks (110 °C, 200 °C and 250 °C). The full analysis is given in the supplement.

Figure 9 shows the results for 110 °C TL peak. The peak intensities are slightly positively skewed, but without any extreme value. IRSL signal and 110 °C TL peak intensities are not correlated ($r = 0.132$), while a positive correlation ($r = 0.945$) was observed for blue-OSL and 110 °C TL peak intensity, as expected from previous investigations (e.g., Aitken & Smith, 1988; Murray & Roberts, 1998; Kiyak et al., 2008). In contrast, for UV TL peaks at higher temperatures (200 °C and 250 °C) IRSL and blue-OSL are positively correlated with the corresponding TL peak intensities (Figs. 10 and 11). Mineral phases other than

quartz may cause this signal correlation, although the TL peaks show no obvious contamination by, e.g., K or Na-feldspar.

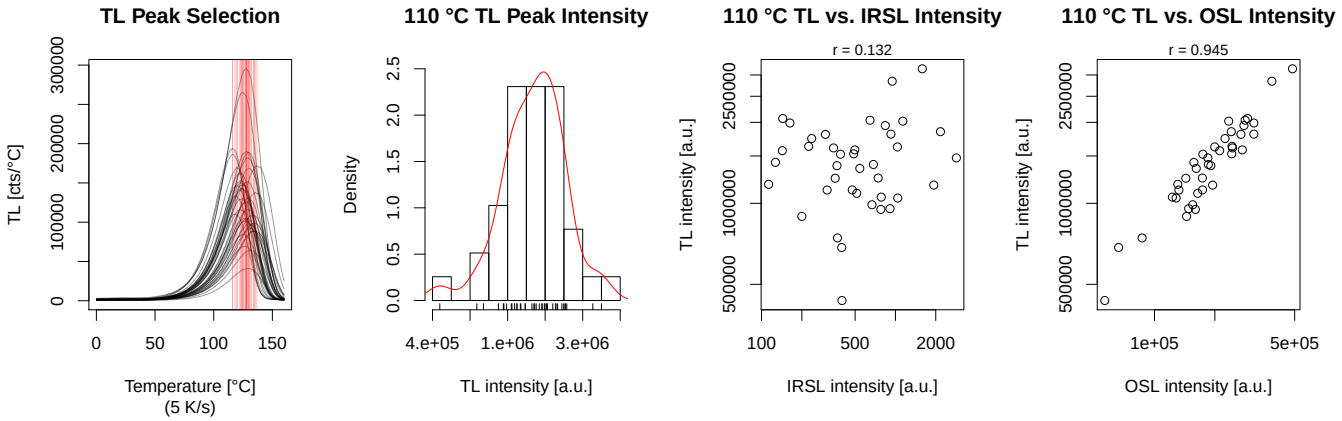

Figure 9. 110 °C TL peak intensity plots. Shown are (left to right): (1) all measured 110 °C TL peaks (cf. Fig. 7B) with identified peak positions marked with red vertical lines, (2) histogram of the logarithmised intensity of the 110 °C peak (peak ± 5 channels), (3) scatter plot of the logarithmised TL peak intensity vs the logarithmised IRSL intensity, (4) scatter plot of the logarithmised 110 °C TL peak intensity vs the logarithmised OSL intensity. The 110 °C TL peak intensity correlates positively with the OSL intensity ($r = 0.95$), while no correlation was found between 110 °C TL peak intensity and the IRSL intensity ($r = 0.13$).

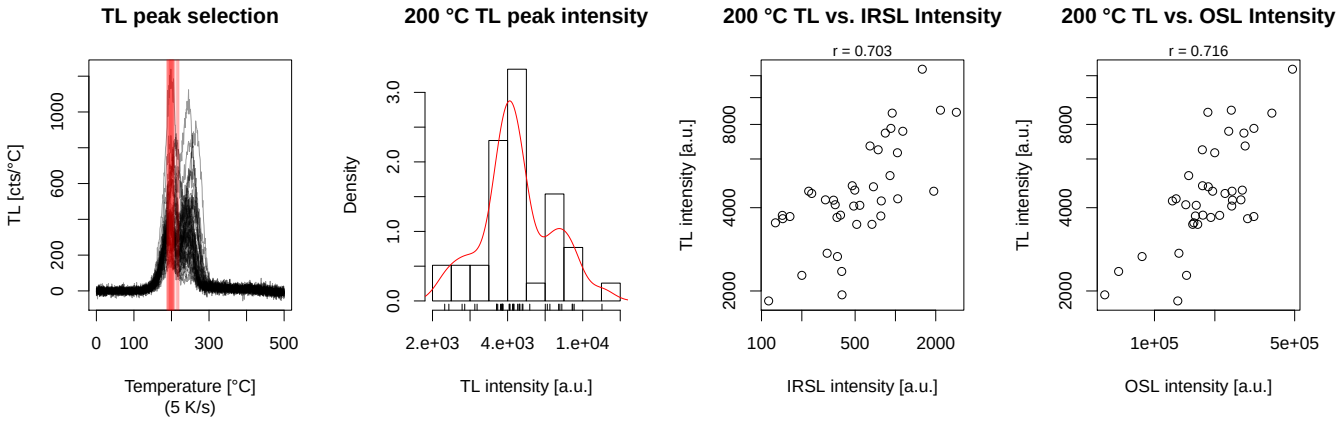

Figure 10. 200 °C TL peak intensity plots. The figure has a similar structure as Fig. 9 and the TL curves (first plot) refer to the results presented in Fig. 7E. It appears that the logarithmised TL peak intensities positively correlate with the logarithmised IRSL and OSL intensities (r values given as subtitles). However, the partly automatic peak selection algorithm might have biased the results since the peak search range was preset and thus the peaks manually predefined.

7. OSL laser scanning

To give a preliminary view of the extent of homogeneity at grain to grain level a pattern of grains was dispensed on a stainless steel disc, β-irradiated with approximately 20 Gy dose, preheated for 30 min at 50 °C and than subjected to OSL laser scanning using the system described by Sanderson et al. (2004). An area of 1 cm^2 was scanned with 1 s OSL data recorded on a 100 μm matrix. Figure 12A shows the resulting colour coded image in pixellated form, Fig. 12B shows a backscattered electron image of the sample disc, indicating the positions of individual grains within the pattern, and Fig. 12C shows the log

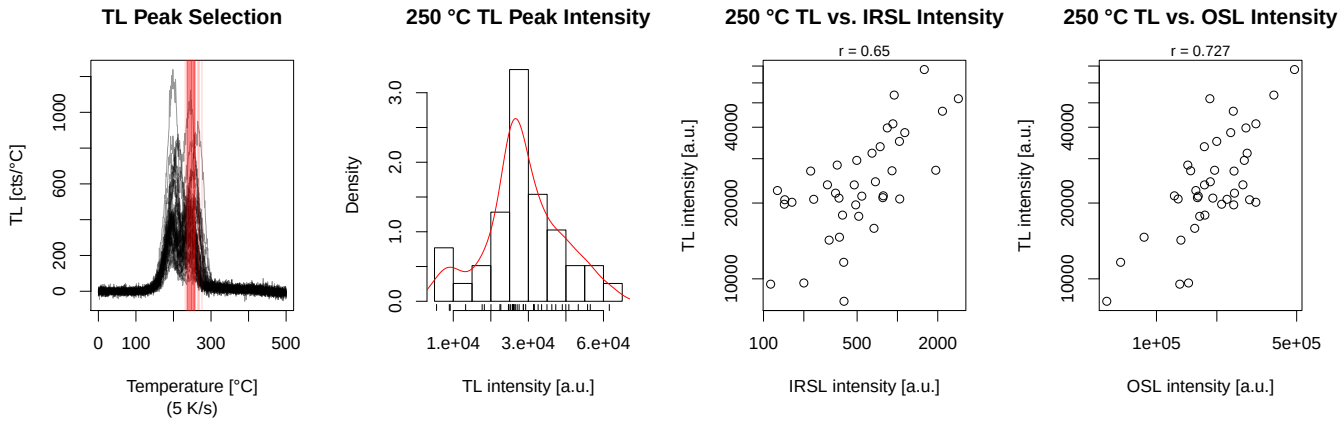

Figure 11. 250 °C TL peak intensity plots. The figure has a similar structure as Fig. 9 and the TL curves (first plot) refer to the results presented in Fig. 7E. As in the previous figure the TL peak intensity appears to correlate with the IRSL and OSL peak intensities. However, also in this case the observed correlation could be an artefact of the partly pseudo-automatic peak selection.

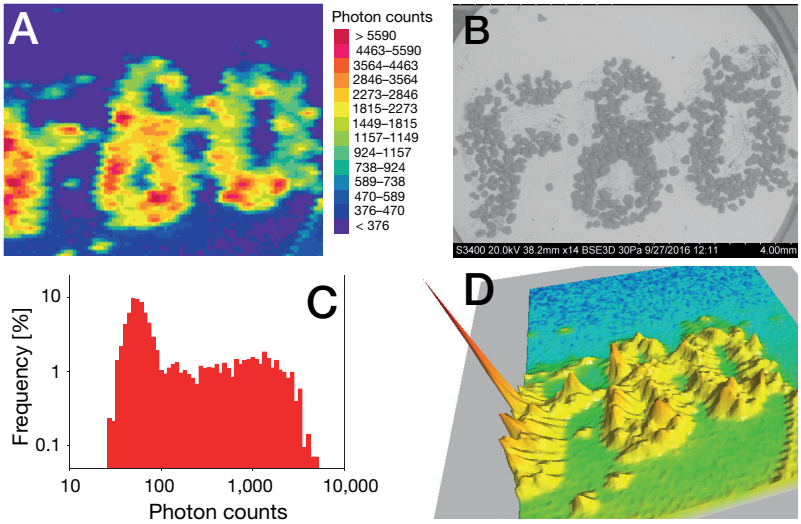

Figure 12. (A) OSL scan of a pattern of Fontainebleau quartz irradiated with a 20 Gy β-dose, (B) a backscatter SEM image of the object, (C) Histogram of the 4,280 pixels containing the grain image FBQ, (D) 3D view of the scanned image.

frequency distribution of the 4,250 pixels containing the pattern FBQ (Fontainebleau Quartz). Empty pixels form the histogram background peak at ca. 50–100 photon counts, with the distribution from approximately 100 counts to 5,000 counts containing data from grains. Figure 12D shows a 3D view of the same data. The data imply that there is a variation of luminescence response from grain to grain of slightly more than one order of magnitude. Additional studies using single grain readers would be needed to characterise this further.

8. ICP-MS analysis

Along with the luminescence screening, for one subsample (FB2A) ICP-MS analyses were carried out at IRAMAT-CRP2A in Bordeaux. The analyses aimed at identifying and quantifying trace elements in the sample. The 1.38 g of sample material were conditioned for the ICP-MS measurement applying HCl (12 mol/l) and HNO_3 (16 mol/l). The solution was further prepared using 3 cycles of treatment with HF (40 %, 3 ml) and $HClO_4$ (72 %, 1 ml).

Table 2. ICP-MS results sample FB2A

Element	Concentration [ppm]
K	35.0 ± 1.2
Th	0.333 ± 0.015
U	0.149 ± 0.007

The results of the ICP-MS analysis are listed in Table 2. In contrast to the previously carried out high-resolution γ-ray spectrometry (100 g), the amount of investigated material is small and variations due to the subsampling are likely. Th concentrations are in agreement with the findings from the γ-ray spectrometry (0.337 ± 0.056 ppm), but still circa twice as high as the average value reported by Vandenberghe et al. (2008) for purified quartz. The U concentration obtained by ICP-MS for the sample (not to be mixed up with internal trace element concentration of 'pure' quartz grains) is an order of magnitude higher than reported by Vandenberghe et al. (2008). However, similar or even higher U concentrations for chemically untreated and treated samples were found by Mejdahl (1987); De Corte et al. (2006) and Steup (2015). Furthermore, the γ-ray spectrometry results (Table 1) indicate that the U concentration for larger sample sizes is an order of magnitude lower (0.061 ± 0.016 ppm). Thus, it appears likely that the few zircon inclusions contribute to the U concentration found by the ICP-MS analysis, which could perhaps be verified by sequential digestion or spatially resolved analysis if needed in the future. The K concentration is consistent with the observations from SEM analysis. The γ-ray spectrometry results (Table 1) list a larger K concentration (190 ± 140 ppm), which appears to be more robust and consistent with XRF data on Fontainebleau Sandstone by Saadi et al. (2017) (K_2O: 140 ± 4 ppm). Nevertheless, our findings confirm the high purity of the quartz sample and suggest that the sample does not contain significant quantities of K-feldspar.

9. Conclusions

A workflow to check purity and appropriate luminescence behaviour of a natural reference quartz sample from the Fontainebleau Sandstone Formation was presented. The preparation and analyses comprised sieving, magnetic separation, optical microscopy, SEM, ICP-MS, γ-ray spectrometry and luminescence screening.

The Fontainebleau quartz consists mainly of Si and O. No significant contamination by other minerals was found in SEM analysis apart from some microinclusions of zircon and rutile and in a few grains some surficial calcium-bearing phases. The bulk K concentrations of only 35 ± 1.2 ppm (ICP-MS) and 190 ± 140 ppm (γ-ray spectrometry on 100 g) indicates no apparent contamination with K-feldspar. However, observed IRSL signals suggest negligible (IRSL/OSL ratio $< 1\,\%$ in 39 out of 40 cases) UV signal contribution by mineral phases other than quartz (e.g., zircon). Luminescence screening confirmed the high luminescence sensitivity for the 110 °C TL peak for low doses (here: 2 Gy) expected from the preselection work, as well as the presence of the other two low-temperature pre-dose sensitivity peaks. Two further UV TL peaks at 200 °C and 250 °C were identified. Glow curve shapes are generally well reproduced, with peak position variations observed in rapid screening measurements on the Risø reader attributed to thermal contact variations. OSL sensitivities are in the order of 10^5 (cts s^{-1}) Gy^{-1} after a TL preheat to 160 °C and IRSL stimulation for 20 s.

The intensity variations from aliquot to aliquot have been defined here and provide a baseline for future assessments of

interlaboratory variations. Sensitivity variations at single grain level have yet to be determined in detail but are implicit in the results of preliminary luminescence scanning work, which suggests grain to grain variations covering at least one order of magnitude. Grain textural (rounded, sub-rounded, sub-angular) differences have been noted in the SEM data, but they appear to be consistent with other work published on the Fontainebleau Sandstone Formation. Overall we conclude that the reference sample is well suited for further analyses within the collaborative group, and have started looking at the 110 °C TL peak characteristics, as well as at individual examinations of other properties.

Acknowledgements

We are thankful to André Sawakuchi for his constructive and thoughtful review. We acknowledge the support of the Bavarian Research Alliance (BayFor) for financing the project meeting in Bayreuth (BayIntAn_UBT_2016_74). JF is gratefully supported by the DFG (2015–2018, "Modelling quartz luminescence signal dynamics relevant for dating and dosimetry", SCHM 3051/4-1). The work of SK is financed by a programme supported by the ANR - n° ANR-10-LABX-52. SUERC provided the material and supported the characterisation and purification work.

References

Adamiec, G. *Investigation of a numerical model of the pre-dose mechanism in quartz*. Radiation Measurements, 39(2): 175–189, 2005.

Aitken, M J and Smith, B W. *Optical dating: recuperation after bleaching*. 7: 387–393, 1988.

Bailey, R M. *The slow component of quartz optically stimulated luminescence*. Radiation Measurements, 32(3): 233–246, 2000.

Bouniol, M. *Les sables de Fontainebleau*. mines et carrières, 199: 16–20, 2013.

Bourbie, T and Zinszner. *Hydraulic and acoustic properties as a function of porosity in Fontainebleau Sandstone*. Journal of Geophysical Research, 90(B13): 11524–11532, 1985.

Bray, H E, Bailey, R M, and Stokes, S. *Quantification of cross-irradiation and cross-illumination using a Risø TL/OSL DA-15 reader*. Radiation Measurements, 35(3): 275–280, 2002.

Burow, C. *calc_AliquotSize(): Estimate the amount of grains on an aliquot. In: Kreutzer, S., Dietze, M, Burow, C, Fuchs, M C, Schmidt, C, Fischer, M, Friedrich, J (2017). Luminescence: Comprehensive Luminescence Dating Data Analysis. R package version 0.7.5.* CRAN, version 0.3.1, 2017. URL https://CRAN.R-project.org/package=Luminescence.

De Corte, F, Vandenberghe, D, Buylaert, J P, Van den haute, P, and Kučera, J. *Relative and k0-standardized INAA to assess the internal (Th, U) radiation dose rate in the "quartz coarse-grain protocol" for OSL dating of sediments: Unexpected observations*. Nuclear Instruments and Methods in Physics Research Section A: Accelerators, Spectrometers, Detectors and Associated Equipment, 564(2): 743–751, 2006.

El Bied, A, Sulem, J, and Martineau, F. *Microstructure of shear zones in Fontainebleau sandstone*. International Journal of Rock Mechanics and Mining Sciences, 39(7): 917–932, 2002.

Friedrich, J, Pagonis, V, Chen, R, Kreutzer, S, and Schmidt, C. *Quartz radiofluorescence: a modelling approach*. Journal of Luminescence, 186: 318–325, 2017.

Gong, Z, Sun, J, Lü, T, and Tian, Z. *Investigating the optically stimulated luminescence dose saturation behavior for quartz grains from dune sands in China*. Quaternary Geochronology, 22: 137–143, 2014.

Grisoni, J-C and Thiry, M. *Réparation des grès dans les sables de Fontainebleau: Implications géotechniques des études récentes*. Bulletin des laboratoires des ponts et chaussées, 157, 1988.

Keleş, Ş K, Meriç, N, and Polymeris, G S. *Dose response on the 110°C thermoluminescence peak of un-heated, synthetic Merck quartz*. Physica B: Physics of Condensed Matter, pp. 1–30, 2016.

Kiyak, N G, Polymeris, G S, and Kitis, G. *LM-OSL thermal activation curves of quartz: Relevance to the thermal activation of the 110∘C TL glow-peak*. Radiation Measurements, 43(2-6): 263–268, 2008.

Kreutzer, S, Schmidt, C, Fuchs, M C, Dietze, M, Fischer, M, and Fuchs, M. *Introducing an R package for luminescence dating analysis* . Ancient TL, 30(1): 1–8, 2012.

Kreutzer, S, Burow, C, Dietze, M, Fuchs, M C, Schmidt, C, Fischer, M, and Friedrich, J. *Luminescence: Comprehensive Luminescence Dating Data Analysis*. CRAN, version 0.7.5, 2017. URL https://CRAN.R-project.org/package=Luminescence. Developer version on GitHub: https://github.com/R-Lum/Luminescence.

Mejdahl, V. *Internal radioactivity in quartz and feldspar grains*. Ancient TL, 5(2): 10–17, 1987.

Murray, A S and Roberts, R G. *Measurement of the equivalent dose in quartz using a regenerative-dose single-aliquot protocol*. Radiation Measurements, 29(5): 503–515, 1998.

Porat, N. *Use of magnetic separation for purifying quartz for luminescence dating*. Ancient TL, 24(2): 33–36, 2006.

Porat, N, Faerstein, G, Medialdea, A, and Murray, A S. *Re-examination of common extraction and purification methods of quartz and feldspar for luminescence dating*. Ancient TL, 33(1): 22–30, 2015.

Powers, M C. *A New Roundness Scale for Sedimentary Particles*. Journal of Sedimentary Petrology, 23(2): 117–119, 1953.

R Core Team. *R: A Language and Environment for Statistical Computing*. Vienna, Austria, 2017. URL http://www.r-project.org.

Robin, A-M and Barthélemy, L. *Essai de chronologie – depuis 2300 ans – de dépôts sableux, pédogénisés, en foret de Fontainebleau (France)*. Comptes Rendus de l'Académie des Sciences - Series IIA - Earth and Planetary Science, 331(5): 359–366, 2000.

Saadi, F Al, Wolf, K-H, and Kruijsdijk, C van. *Characterization of Fontainebleau Sandstone: Quartz Overgrowth and its Impact on Pore-Throat Framework*. Journal of Petroleum & Environmental Biotechnology, 08(03): 1–12, 2017.

Sanderson, D C W, Carmichael, L A, and Fisk, S. *Thermoluminescence Detection of Irradiated Fruits and Vegetables: International Inter-laboratory Trial*. Journal of AOAC International, 86(5): 971–975, 2003a.

Sanderson, D C W, Carmichael, L A, and Fisk, S. *Thermoluminescence Detection of Irradiated Shellfish: International Interlaboratory Trial*. Journal of AOAC International, 86(5): 976–982, 2003b.

Sanderson, D C W, Carmichael, L A, and Fisk, S. *Photostimulated Luminescence Detection of Irradiated Shellfish: International Interlabo-ratory Trial*. Journal of AOAC International, 86(5): 983–989, 2003c.

Sanderson, D C W, Carmichael, L A, and Fisk, S. *Photostimulated Luminescence Detection of Irradiated Herbs, Spices, and Seasonings: International Interlaboratory Trial*. Journal of AOAC International, 86(5): 990–997, 2003d.

Sanderson, D C W, Carmichael, L A, Murphy, S D, Whitley, V H, Scott, E M, and Cresswell, A J. *Statistical And Imaging Methods For Luminescence Detection Of Irradiated Ingredients*. Food Standards Agency Research Report, Reference CSA 5240: 40p, 2004.

Steup, R. *Charakterisierung von natürlichen Quarz-Präparaten unterschiedlicher Genese und Herkunft unter Anwendung von Techniken zur Elementanalyse*, 2015. unpublished Bachelor's thesis (in German), University of Gießen.

Thiry, M and Marechal, B. *Development of Tightly Cemented Sandstone Lenses in Uncemented Sand: Example of the Fontainebleau Sand (Oligocene) in the Paris Basin*. Journal of Sedimentary Research, 71(3): 473–483, 2001.

Thiry, M, Ayrault, M B, and Grisoni, J-C. *Ground-water silicification and leaching in sands: Example of the Fontainebleau Sand (Oligocene) in the Paris Basin*. Geological of America Bulletin, 100: 1283–1290, 1985.

Vandenberghe, D, De Corte, F, Buylaert, J P, Kučera, J, and Van den haute, P. *On the internal radioactivity in quartz*. Radiation Measurements, 43(2-6): 771–775, 2008.

Wintle, A G and Murray, A S. *The relationship between quartz thermoluminescence, photo-transferred thermoluminescence, and optically stimulated luminescence*. Radiation Measurements, 27(4): 611–624, 1997.